IOPscience iopscience.iop.org

Home Search Collections Journals About Contact us My IOPscience

Determination of interatomic distances and coordination numbers by K-XANES in crystalline minerals with distorted local structure

This article has been downloaded from IOPscience. Please scroll down to see the full text article.

2000 J. Phys.: Condens. Matter 12 1119

(http://iopscience.iop.org/0953-8984/12/6/328)

View the table of contents for this issue, or go to the journal homepage for more

Download details:
IP Address: 171.66.16.218
The article was downloaded on 15/05/2010 at 19:54

Please note that terms and conditions apply.

J. Phys.: Condens. Matter **12** (2000) 1119–1131. Printed in the UK PII: S0953-8984(00)05758-1

Determination of interatomic distances and coordination numbers by K-XANES in crystalline minerals with distorted local structure

L A Bugaev†, Ph Ildefonse‡, A M Flank§, A P Sokolenko† and H V Dmitrienko†

† Department of Physics, Rostov University, Zorge str. 5, Rostov-on-Don 344090, Russia
‡ Laboratoire de Mineralogie-Cristallographie, UA CNRS 09, Universites Paris 6 et 7, and IPGP, 4 place Jussieu, 75252 Paris cedex 05, France
§ LURE, CNRS/CEA/MEN, Bat. 209D, 91405 Orsay, France

Received 6 July 1999, in final form 15 October 1999

Abstract. The method for quantitative determination of interatomic distances and coordination numbers (CN) from experimental K-XANES of light metallic atoms in crystalline compounds with distorted local structure is proposed, based on the extraction of the first shell term and the multiple-scattering term. In crystalline minerals the extraction of these terms can be obtained under uncertainties of ∼0.3–0.4 Å in the values of the second and more distant shell radii, using the unambiguous diffraction data on cell unit parameters and the type of point symmetry. The fitting of the extracted first shell term by theoretical terms, generated within alternative models for the split of this shell under the local structure distortions in the environment of the absorbing metallic atom, permits one to obtain the interatomic distances and CN in reasonable quantitative agreement with the diffraction data for the reference compounds studied.

1. Introduction

During the last few years, x-ray absorption spectroscopy (XAS) has been extensively used for local structure determination in disordered systems. It was revealed [1, 2] that interpretation and analysis of the absorption spectra fine structure (XAFS) appears to be the most reliable approach for identifying the local structure distortions, when the traditional diffraction methods are not sensitive to short-range structure, or can give only the values of averaged atomic positions in the lattice. However, the unknown structure parameters—interatomic distances (R), bond angles and coordination numbers (CN) are usually extracted from the extended fine structure of the spectrum (EXAFS), while the near-edge region (XANES), which is very sensitive to the type of absorbing atom coordination [3, 4] and contains much more structure information, is used for qualitative analysis only. The main reasons for these limitations were discussed in [5] and arise from the application of the widely available full multiple-scattering approach to XANES description [6–9]. This approach permits one to reproduce the spectrum features in agreement with the experiment for atomic systems with an exactly known structure, when the atom positions are unambiguously determined by diffraction methods, but appear to be of no use to solve the inverted problem—quantitative determination of local structure parameters, when the uncertainty in the diffraction data interpretation takes place or these data are unavailable. In this case, the structure information could be obtained from EXAFS. However, EXAFS-oscillations often cannot be experimentally obtained due to either measurement conditions, or

0953-8984/00/061119+13$30.00 © 2000 IOP Publishing Ltd

the nature of the compounds studied. Therefore, for such compounds, the XANES spectra are the most widely available source of information on their local atomic structure.

As was discussed in [5], the inverted problem solution—determination of local structure parameters by XANES—can be obtained using the description of the approach to XANES, based on the treatment of photoelectron single-scattering (SS) on two-atom chains A–S (A—absorbing, S—environment atoms) and low-angle double- (DS) and triple-scattering (TS) processes on approximately linear three-atom chains A–F–S (F—intermediate atom), originated at the absorbing atom A. The validity of this EXAFS-like approach to the XANES description was justified in [5] by Al K-XANES spectra calculations in a number of Al containing minerals with distorted structure and different coordination of the absorbing Al-atom. In the present paper, the approach and the generated XAFS and SELCOMP codes [5] are applied to describe Mg K-XANES in minerals with different CN of Mg (section 2): spinel ($MgAl_2O_4$, with fourfold coordinated Mg) and pyrope ($Mg_3AlSi_3O_{12}$, with eightfold coordinated Mg). The agreement of the theoretical Al and Mg K-XANES with the experimental results, justifies the validity of the EXAFS-like approach to describe these spectra for a wide number of minerals which consist of light atoms. This permits us to propose a method for CN and interatomic distances determination in crystalline compounds with local distortions, when uncertainties in the diffraction data interpretation occur. A description of the method, based on the extraction of the first shell term from experimental XANES of the compound, is given in section 3 and 4 using the following reference minerals with known atomic structures, analysed in [5]: berlinite ($AlPO_4$, with fourfold coordinated Al) and pyrophyllite ($Al_2(Si_4O_{10})(OH)_2$, with sixfold coordinated Al). For these compounds, the contribution into XANES from the oxygen atoms, nearest to the absorbing Al-atom (split O-tetrahedron in berlinite and split O-octahedron in pyrophylite), is extracted from the experimental Al K-XANES spectrum. The fitting procedure, described in section 5, permits one to obtain the corresponding distances and CN, which characterize the split, in quantitative agreement with the diffraction data available.

The significance of the proposed method can be traced, on the one hand, from atomic position determination in crystalline compounds with local disorder, when the diffraction methods give reliable values of cell parameters and the type of point symmetry. At the same time, however, there are ambiguities in the atomic positions in the unit and, as a result, uncertainty in the radial distribution of the atoms in the vicinity of the absorbing atom. This problem is now solved for ABO_3 crystals, when the small atomic displacements from the symmetric positions are determined and the results obtained by this method are additional to those obtained by EXAFS [10]. On the other hand, the main points of the proposed method (except to restore the SS contribution from the second and more distant shells) can be retained and are used now within the proposed method for quantitative determination of local structure parameters in amorphous compounds which consist of light atoms. For these compounds only qualitative analysis is possible now, comparing their XANES features with the similar features of the reference compounds.

2. The method of spectra calculation and Mg K-XANES in pyrope and spinel within the EXAFS-like approach

The experimental Mg K-XANES spectra in pyrope (CN $=$ 8) and spinel (CN $=$ 4) are characterized by significant differences in the light features at low energies [11]. The diffraction data available [12, 13] permit one to reproduce the atomic structure of the absorbing Mg-atom environment and to carry out direct *ab initio* calculations of the spectra. The obtained theoretical Mg K-XANES of pyrope and spinel are compared with the experimental spectra in figure 1. The presented spectra were calculated according to the approach proposed in [5],

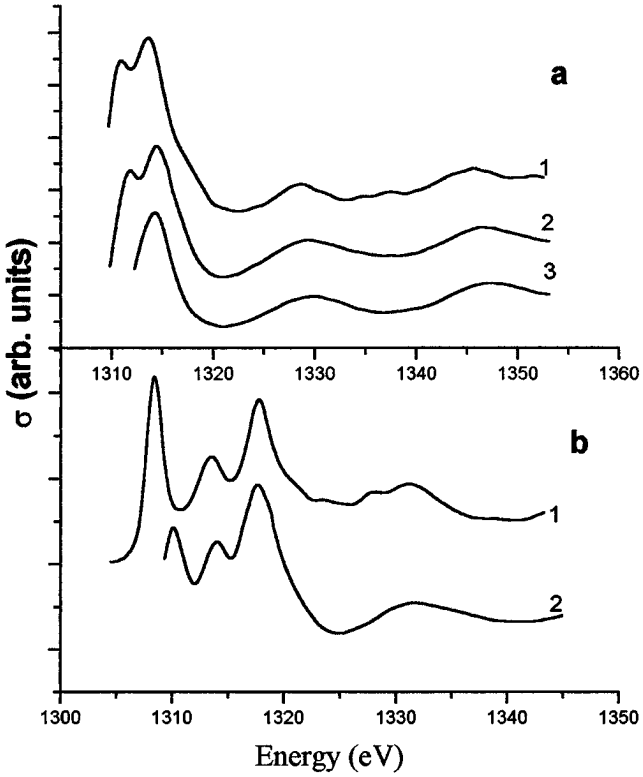

Figure 1. Experimental (curves 1) and theoretical (curves 2) Mg K-XANES spectra of (a) pyrope (CN = 8) and (b) spinel (CN = 4). Curve 3 in (a) corresponds to the SS-approximation.

using the expression for the absorption cross-section of an atom in the compound:

$$\sigma(\varepsilon) = \sigma_{at}(\varepsilon)[1 + \chi(\varepsilon)] \tag{1}$$

where ε is the photoelectron energy initiated from the interstitial potential, known as the muffin-tin (MT) zero, i.e. $\varepsilon = E - E_{MT}$. $\sigma_{at}(\varepsilon)$ is the factorized part of the absorption cross-section, contains the matrix element for 1s-photoionization $\sim|\langle 1s|\nabla|\varepsilon\ p\rangle|^2$ and the contribution of the accompanied intrinsic processes within the absorbing atom. The $\chi(\varepsilon)$ is the total contribution into $\sigma(\varepsilon)$ from the photoelectron scattering processes on environment atoms, determined by the expression:

$$\chi(\varepsilon) = \chi_{SS}(\varepsilon) + \sum_{i=1}^{p}[\chi_2^{(i)}(\varepsilon) + \chi_3^{(i)}(\varepsilon)] = \chi_{SS}(\varepsilon) + \chi_{MS}(\varepsilon) \tag{2}$$

where $\chi_{SS}(\varepsilon)$ is the contribution of the SS processes on two-atom chains, $\chi_2^{(i)}(\varepsilon)$, $\chi_3^{(i)}(\varepsilon)$ are, respectively, the double- and triple-scattering terms on ith chain A–F–S, p is the total number of these chains, chosen under the empirical selection rule, which consists of A_{min}, the angle parameter of chains ($A_{min} = 1.0$ for linear chains) and R_{max}, the maximum value of the scattering pathway length in the compound [5]. The selection rule is obtained for every structure studied through the fitting of an experimental spectrum using a theoretical one, carried out using the SELCOMP code. The values obtained for the parameters are: $R_{max} = 16.6$ Å, $A_{min} = 0.92$ for pyrope and $R_{max} = 13.3$ Å, $A_{min} = 0.97$ for spinel, i.e.,

the approximately linear chains within the clusters with radii $R_{max}/2$ must be considered for XANES calculations. The expressions for χ_{SS}, χ_2 and χ_3, obtained through the spherical wave formalism, can be found in [14] and are realized in the XAFS code. In the following, the sum of the terms $\chi_2(\varepsilon)$ and $\chi_3(\varepsilon)$ in equation (2) is noted as a multiple-scattering (MS) term, $\chi_{MS}(\varepsilon)$.

The phase shifts for photoelectron scattering on atoms in the compounds studied were calculated using the method of Hartree–Fock (HF) MT-potential generation [15, 16]. This method permits one to obtain theoretical XANES and EXAFS spectra systematically, in agreement with the experimental spectra [2, 14–16]. With the help of this method, high accuracy for structure parameters of the first shell in metals is obtained from EXAFS data analysis, using the calculated phase shifts and scattering amplitudes [17]. The advantages of the HF MT-potential model used, compared to other models, are: (a) the simplicity of the potential generating procedure, which provides the energy independent interstitial potential value E_{MT}, used as the initial photoelectron energy or wave number instead of the traditional adjustable parameter E_0; (b) it does not need any preliminary knowledge of the nearest shell distances or coordination numbers; (c) if necessary, the charges of the atoms in the compound can easily be included within this model [18].

The MT approximation normally used, as well as accounting for multielectron excitations—intrinsic losses by the undetermined energy-dependent reduction factor $S_0^2(\varepsilon)$ [19]—make the theoretical function $\sigma_{at}(\varepsilon)$, obtained through the direct *ab initio* calculations in the near edge energy region, unreliable. Therefore, $\sigma_{at}(\varepsilon)$ was obtained from the experimental XANES spectrum of the compound studied by the developed procedure [20]. This was based on the smearing of $\sigma^{exper}(\varepsilon)$ under large, nonphysical values of core hole energy width Γ and then the recovery of $\sigma_{at}(\varepsilon)$ under this Γ value. The accuracy of the proposed procedure was tested for different reference minerals, consisting of light atoms, by comparing their theoretical XANES with the experimental results. The $\sigma_{at}(\varepsilon)$ obtained are used in the following (section 4) to extract the first shell term from the experimental XANES. The photoelectron extrinsic losses were taken into account through the traditional exponential form $\exp(-R/\lambda(\varepsilon))$. The photoelectron mean free path length $\lambda(\varepsilon)$ is usually not known exactly, especially for the near edge region of the spectrum. However, the model XANES calculations, carried out with different $\lambda(\varepsilon)$ dependencies, varied around the so-called universal curve for monatomic compounds [21] and did not significantly change the spectrum fine structure obtained. Therefore, the smooth energy dependencies for $\lambda(\varepsilon)$ were chosen so as to adjust the envelope of the experimental spectrum. XANES calculations were performed using the approximation for the Debye–Waller (DW) factor, $\exp(-2\sigma^2k^2) \approx 1.0$, suitable within the short range of small XANES energies from $\varepsilon = 0.5$ to 2.2 Ryd above the MT zero or corresponding k values from 1.35 to 2.7 Å^{-1}, when the DW factor remains $\geqslant 0.9$ under variations in the DW parameter $2\sigma^2$ up to ~ 0.15 Å^2.

The agreement obtained with the experimental spectra for Mg K-XANES is presented in figure 1, as well as the Al K-XANES in a wide range of minerals [5], calculated by the method described above. This justifies the adequacy of XANES interpretation in compounds, consisting of light atoms, as a sum of SS and low-angle MS-processes on two- and approximately linear three-atom chains, originated at the absorbing atom, i.e., within the EXAFS-like approach. As a result, in the following, a procedure for structure parameters determination, similar to that used for EXAFS, is proposed for XANES of crystalline compounds with local structure distortions, based on the proposed method, which permits one to overcome the difficulties in the Fourier-analysis of $\chi(k)$ functions within the short XANES k range.

3. Description of photoelectron SS processes on the second and more distant shells in distorted crystalline structures

The quantitative determination of local structure parameters by XAFS can be performed if the EXAFS region of the spectrum is available. In this case, the Fourier-transformation (FT) of $\chi(k)$ in the wide k range, from $k_{min} \sim 3$ to $k_{max} \sim 12$–14 Å^{-1}, results in $|F(R)|$ with narrow peaks, which correspond to the shells in the environment of the absorbing atom. Moreover, the first shell peak is usually well separated from the peaks of the second and more distant shells, so its fitting permits one to obtain precise values of corresponding structure parameters. The problem becomes complicated for crystalline and amorphous compounds, which consist of light atoms ($Z \leqslant 20$), because, as was mentioned above, EXAFS oscillations often cannot be observed and only the XANES spectrum is available. Calculations for the reference compounds show that in this case the $\chi(k)$ can also be extracted from the experimental XANES, according to (1), using the obtained σ_{at}. However, the FT of $\chi(k)$ within the short XANES k range, from $k_{min} = 1.35$ to $k_{max} = 2.7$ Å^{-1}, results in the broad first shell peak (up to ∼5 Å, section 4), which overlaps the region of the radii for the second and more distant shells. At the same time, the calculations performed revealed that the peaks in $|F(R)|$, arising from the MS processes, are located at $R \geqslant 6$–7 Å due to the long pathway length and hence, are well separated from the first shell peak. Therefore, if for the compound studied one can theoretically restore the contribution of the photoelectron SS processes on the second and more distant shells (long-range order term, χ_{SS}^{LRO}) and extract it from $\chi(k)$, then the sum of the low-frequency first shell term ($\chi_{SS}^{(1)}$) and the high-frequency MS term (χ_{MS}), i.e. the function $\chi_{SS}^{(1)} + \chi_{MS}$, can be obtained from the experimental XANES. As a result, the $|F(R)|$ of this sum contains the first shell peak and MS peaks, separated in R-space. So the back Fourier transformation (BFT) of the $F(R)$, performed with corresponding window functions, permits one to obtain the terms $\chi_{SS}^{(1)}$ and χ_{MS} separately and to apply the fitting procedure to $\chi_{SS}^{(1)}(k)$ within the short k range treated (sections 4 and 5). In this section, the theoretical restoration of the χ_{SS}^{LRO} term in a crystalline compound, and with uncertainties in the values of the shell radii which arise from the diffraction data analysis, is proposed. This is illustrated using the reference compounds of berlinite and pyrophyllite [5] with different coordination of the absorbing Al-atom.

The calculations of Al K-XANES [5] and Mg K-XANES spectra in section 2 revealed the importance of accounting for the scattering processes on far atomic shells in the compounds studied. For example, the values of the cluster radii, which must be taken for berlinite and pyrophyllite, are 8.5 and 9.1 Å, respectively. Analysing the distribution of the shell radii R_j (j is the shell's number) for the structures studied, one can find the approximate infinitive distribution of the R_j values, beginning from the second or more distant shells. At the same time, the difference between the first and the second shells may be more than 1 Å. In distorted systems, the CN for these shells can decrease by up to 2 or even 1 atom and therefore the number of shells within the chosen cluster rapidly increases up to several thousands.

In this case one can assume that the SS contribution into XANES from the second and more distant shells (LRO term) can be theoretically reproduced without accurate data on the values of each shell radius R_j—the distance between the jth shell atoms and the absorbing atom. To prove this assumption, the shells in the structures studied were grouped according to the types of atoms in them, with R_j increasing. As a result, the structure studied can be represented by the number of atomic groups obtained, and each ith group contains the shells of only one atom type (for example, O- or Al-atoms), with radii within $\langle R_i \rangle \pm \Delta_i/2$, where $\langle R_i \rangle$ is the averaged radius of the shells in the ith group and $\Delta_i/2$ is the maximum value of the shell radius deviation from $\langle R_i \rangle$. The ith group SS contribution $\chi_{SS}^{(i)}(\varepsilon)$ into XANES is

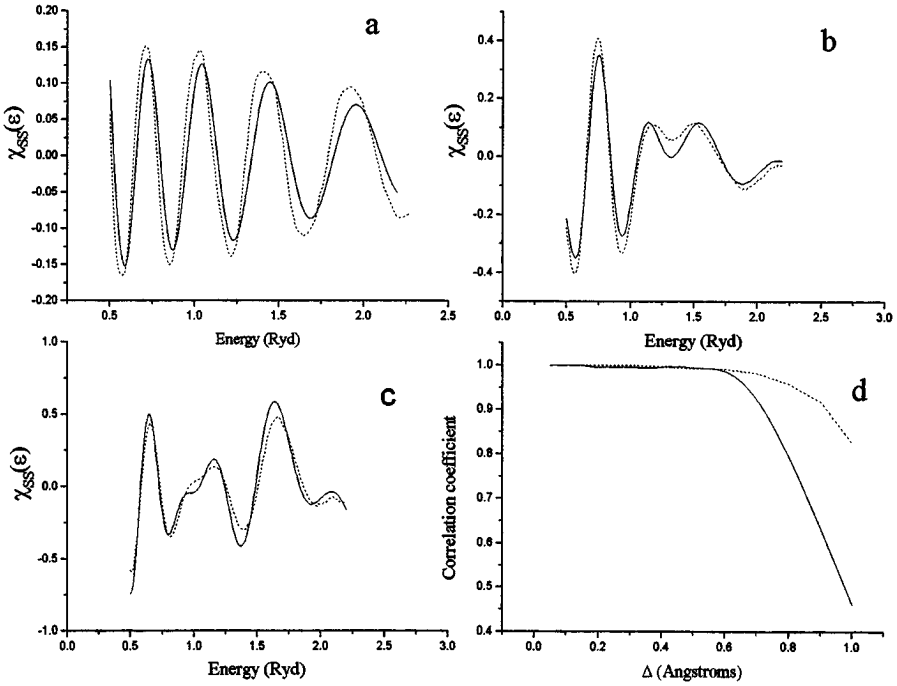

Figure 2. (a) $\chi_{SS}^{(i)}(\varepsilon)$ for the group of 12 oxygen shells: solid curve—calculation by (3) for 12 shells with radii from 7.74 to 8.35 Å ($\Delta = 0.6$ Å); dashed curve—two-atom chain contribution $\chi_{SS}^{(i)}(\varepsilon, \langle R_i \rangle = 8.1$ Å). (b), (c) $\chi_{SS}(\varepsilon)$ from the second and more distant shells calculated exactly (full curves) and by the model of atomic groups, formed under $\Delta = 0.6$ Å (dashed curves), for berlinite (b) and pyrophyllite (c) structures. (d) Correlation coefficient between the exact and approximately calculated $\chi_{SS}(\varepsilon)$ terms as a function of Δ for berlinite, (full curve) and pyrophyllite (dashed curve).

determined by the expression:

$$\chi_{SS}^{(i)}(\varepsilon) = \sum_{j=j_{min}}^{j_{max}} \chi_{SS}^{(j)}(\varepsilon, R_j) \tag{3}$$

where j_{min} and j_{max} are the lower and the upper numbers of the shells included in the ith group. The Δ_i may differ for different groups and their values can be obtained via direct model SS calculations for the types of structures studied. The main problem here is finding the same Δ value for all groups of atoms, which provides the reproduction exactly calculated by (3) of every ith group SS contribution $\chi_{SS}^{(i)}(\varepsilon)$ into XANES, by the single two-atom chain term $\chi_{SS}^{(i)}(\varepsilon, \langle R_i \rangle)$—the contribution of the SS processes on two-atom chain A–S (A—absorbing atom, S—atom of the same type as in the ith group) with the distance $\langle R_i \rangle$ between A and S. The SS calculations carried out for the structures studied, revealed the reproduction of $\chi_{SS}^{(i)}(\varepsilon)$ by $\chi_{SS}^{(i)}(\varepsilon, \langle R_i \rangle)$ when atomic shells are grouped under the Δ value of not more then 0.6 Å. In figure 2(a) the comparison of $\chi_{SS}^{(i)}(\varepsilon)$ calculated by (3) for the group of 12 oxygen shells with radii from 7.74 to 8.35 Å ($\Delta = 0.6$ Å) in the berlinite structure is compared with $\chi_{SS}^{(i)}(\varepsilon, \langle R_i \rangle = 8.1$ Å). A disagreement between the curves, revealed for one atomic group, becomes negligible if we compare the resulting SS contribution from the second and more distant shells, calculated exactly, with the same SS contribution obtained by the model considered for atomic groups, formed under $\Delta = 0.6$ Å. The corresponding curves for the

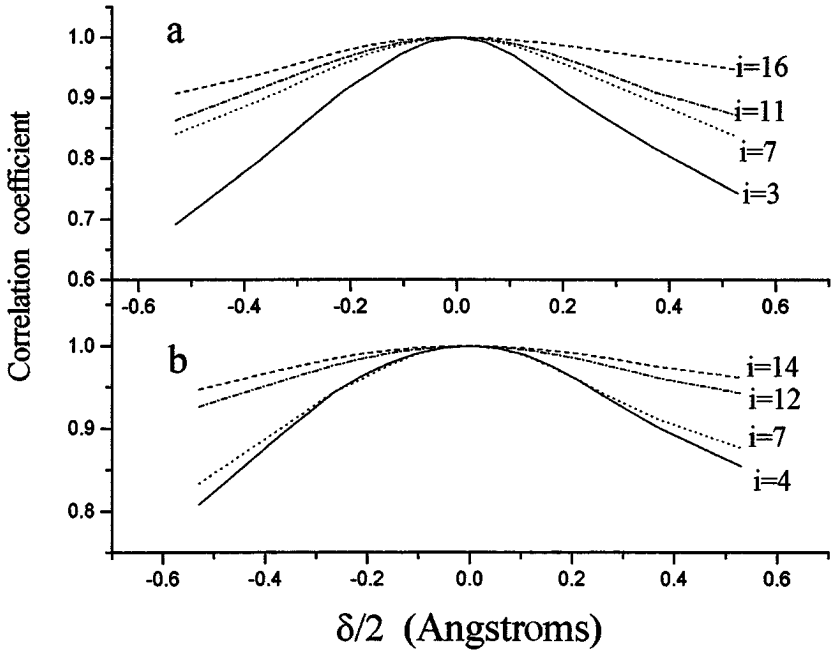

Figure 3. The values of the correlation coefficient for different atomic groups (i, the number of the group) in berlinite (a) and pyrophyllite (b) structures as a function of δ, the uncertainty in the value of the ith atomic group radius $\langle R_i \rangle$.

berlinite and pyrophylite structures, are presented in figures 2(b) and (c) and the quantitative agreement of the χ functions compared is justified by the value of the correlation coefficient (C), presented in figure 2(d) as a function of Δ. The results obtained remain stable when the different atomic groups in the structure are partly overlapped.

The proposed simplified description of the SS contribution of second and more distant shells into XANES may in itself be important for spectra interpretation. However, the main result obtained is that the long-range order SS terms in the structures studied can be reproduced under the uncertainties, δ_i, in the $\langle R_i \rangle$ values. To find the ultimate values for δ_i, the radius of each atomic group in the structure was varied within the ranges $\langle R_i \rangle \pm \Delta_i/2$ and the $\chi_{SS}^{(i)}$ functions, calculated for the chosen radii of the group, were compared with the $\chi_{SS}^{(i)}(\varepsilon, \langle R_i \rangle)$. The comparison was carried out using the value of the correlation coefficient C between the compared functions. The C values for different groups of atoms in berlinite and pyrophylite structures are presented in figure 3 as functions of $\delta/2$. As can be seen, the high C values ($\geqslant 0.9$) for all groups of atoms remain up to $\delta \approx 0.3$–0.4 Å and hence, the same uncertainties in the values of each shell radius R_j are allowable to describe the second and more distant shell contributions (LRO term) into XANES. The result obtained is justified via simulations of the LRO term under direct variations in the shell radii in minerals with different types of point symmetry and CN of the absorbing atom (berlinite, pyrophyllite and pyrope structures), and therefore can be expected to be valid for a wide number of related compounds which consist of light atoms.

The uncertainties δ in the values of the shell radii arise from the uncertainties in the atomic positions in the cell unit and they are of the same order, being connected by simple expression. Therefore, one can conclude that the ultimate values of uncertainties δ in the shell

radii, when the second and more distant shell SS contributions into XANES can be reproduced without exact diffraction data on the atomic positions in the unit, appear to be ∼0.3–0.4 Å in the compounds studied. The radial distribution of atoms in the absorbing atom environment, necessary for SS calculations of the LRO term, can be generated then by, for example, the SEXIE code [22], using the unambiguous diffraction data on the cell parameters and the type of point symmetry.

4. Extraction of the first shell term and MS term from experimental XANES

The calculations of Al and Mg K-XANES in minerals [5, 25] as well as the Mg K-XANES in pyrope and spinel, presented in section 2, revealed the significant effect of photoelectron MS-processes on the spectra fine structure in the energy region $\varepsilon \leqslant$ 15–20 eV, above the absorption threshold. Within the developed method these MS terms can be extracted from the experimental XANES together with the first shell term. The procedure for the first shell term ($\chi_{SS}^{(1)}$) and the MS term (χ_{MS}) extraction from experimental XANES (as well as from EXAFS) spectra can be proposed using the results of section 3 on accounting for SS processes from the second and more distant shells (χ_{SS}^{LRO} term) in a crystalline compound with partial information on its atomic structure. To illustrate this procedure, expression (2) for $\chi(\varepsilon)$ must be rewritten as:

$$\chi(\varepsilon) = \chi_{SS}^{(1)}(\varepsilon) + \chi_{SS}^{LRO}(\varepsilon) + \chi_{MS}(\varepsilon). \tag{4}$$

If the term $\chi_{SS}^{LRO}(\varepsilon)$ can be obtained theoretically, according to the proposals in section 3, then the sum $\chi_{SS}^{(1)}(\varepsilon) + \chi_{MS}(\varepsilon)$ can be extracted from the experimental absorption cross-section $\sigma^{exper}(\varepsilon)$ by the following equation, obtained from (1) and (4):

$$\chi_{SS}^{(1)}(\varepsilon) + \chi_{MS}(\varepsilon) = \sigma^{exper}(\varepsilon)/\sigma_{at}(\varepsilon) - 1 - \chi_{SS}^{LRO}(\varepsilon). \tag{5}$$

The analysis of corresponding theoretical terms on the left side of (5), carried out through direct calculations for the studied reference structures, revealed that $\chi_{MS}(\varepsilon)$ is a high-frequency oscillated term (4–5 oscillations within the energy interval $\varepsilon \leqslant$ 30 eV), while the term $\chi_{SS}^{(i)}(\varepsilon)$ is low-oscillated, because of the small first shell radius R_1. This frequency separation of terms on the left side of (5) permits one to apply the FT procedure to the function $\chi_{SS}^{(1)}(\varepsilon) + \chi_{MS}(\varepsilon)$, extracted by (5) from the experimental Al K-XANES within the small XANES energies or corresponding k range from $k_{min} = 1.35$ to $k_{max} = 2.7$ Å^{-1}. The FT results, $|F(R)|$, of the functions $\chi_{SS}^{(1)}(\varepsilon) + \chi_{MS}(\varepsilon)$ for berlinite and pyrophyllite are presented in figure 4. As can be seen, the $|F(R)|$ for both berlinite and pyrophylite are characterized by the presence of the broad first shell peak and the resulting structure arises from the χ_{MS} term. The last conclusion is justified by the structure of $|F(R)|$, obtained via the FT of the corresponding theoretical χ_{MS} terms only, also shown in figure 4. As can be seen, the two main peaks in the $|F(R)|$ of χ_{MS}, except for their small side lops at lower R values, are separated in R space from the first shell peak. Therefore, the BFT procedure, applied to the $|F(R)|$ of the sum $\chi_{SS}^{(1)} + \chi_{MS}$, with window function at these two main MS peaks, permits one to extract the χ_{MS} term and to compare it with the corresponding theoretical term, directly simulated for the treated reference compounds. This comparison, performed for berlinite and pyrophyllite structures and presented in figure 5, shows the agreement of the χ_{MS} term, extracted by BFT, with the simulated terms. The results obtained permit one: (1) to conclude that the small side lops of the MS signal under the first shell peak in $|F(R)|$ does not significantly affect the accuracy of the Fourier analysis and hence can be ignored; (2) to propose the corresponding procedure for the χ_{MS} term extraction from experimental XANES. The validity of this procedure for a wide number of light atom compounds is justified by the model calculations for different reference

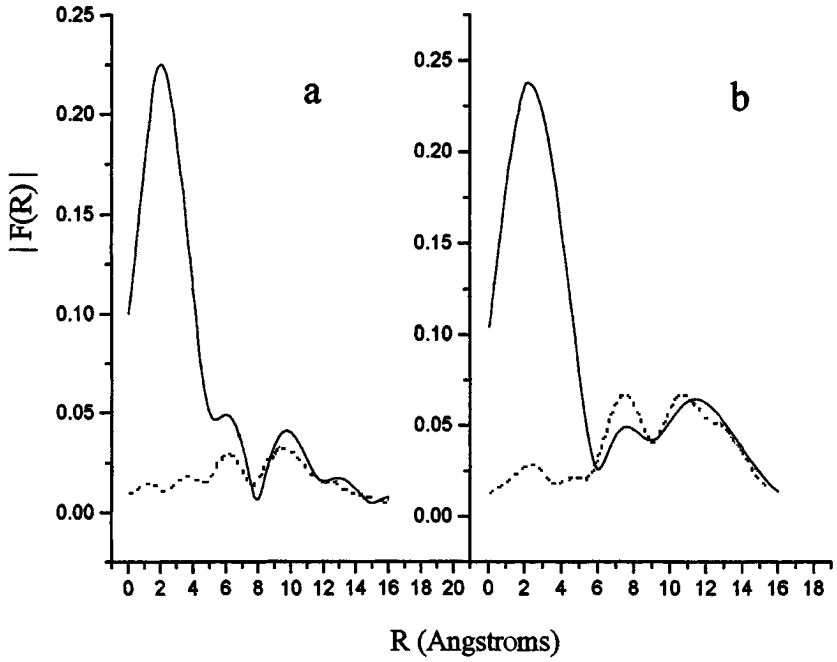

Figure 4. $|F(R)|$ of the function $\chi_{SS}^{(1)} + \chi_{MS}$, extracted using (5) from the experimental XANES (full curves) and of the simulated theoretical terms χ_{MS} (dashed curves), for berlinite (a) and pyrophyllite (b).

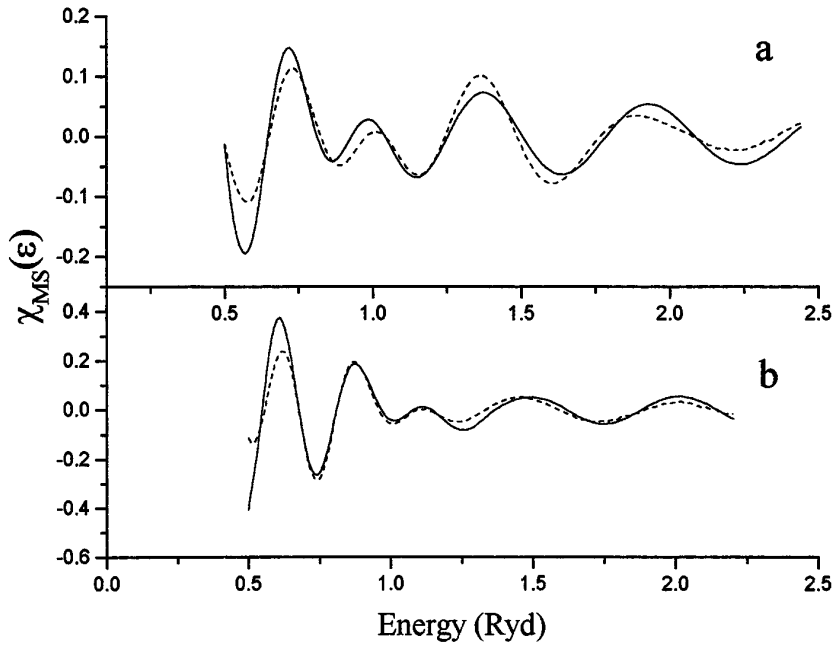

Figure 5. $\chi_{MS}(\varepsilon)$, calculated by the available diffraction data (full curves) obtained by the BFT procedure (dashed curves) from $|F(R)|$ of the function $\chi_{SS}^{(1)} + \chi_{MS}$, extracted using (5) from the experimental XANES for berlinite (a) and pyrophyllite (b).

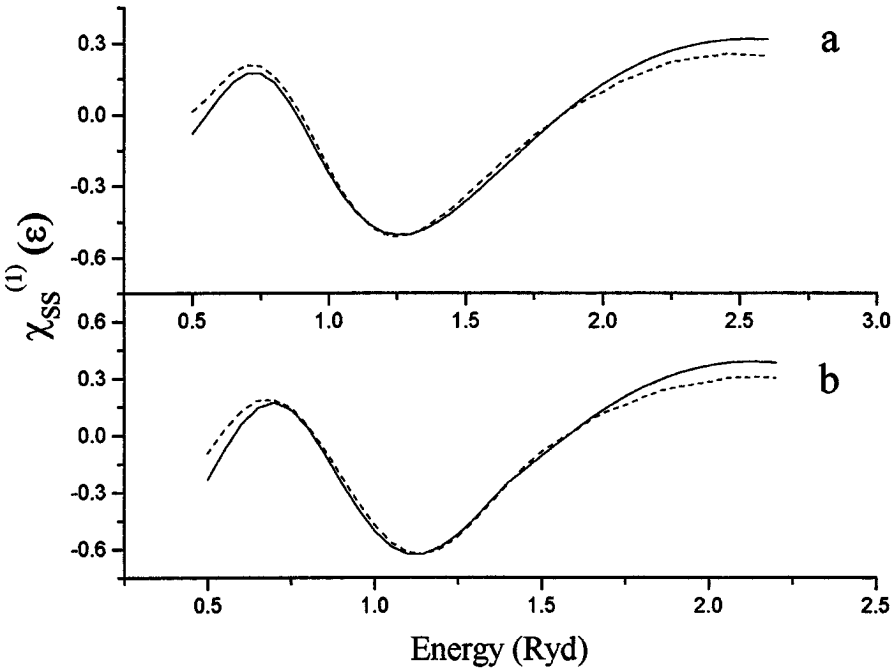

Figure 6. The contribution $\chi_{SS}^{(1)}(\varepsilon)$ into Al K-XANES from the oxygen atoms, nearest to the absorbing the Al-atom: calculated exactly, using the diffraction data on interatomic distances and CN (full curves) and obtained from $|F(R)|$ of the function $\chi_{SS}^{(1)} + \chi_{MS}$, extracted using (5) from experimental Al K-XANES (dashed curves), for berlinite (a) and pyrophyllite (b).

structures [5] and is based on the results, which prove that the χ_{MS} terms in these structures are formed under approximately the same 'selection rules' for three-atom chains, to be considered for XANES calculations.

The revealed separation of the first shell peak and the MS peaks in the $|F(R)|$ of the sum $\chi_{SS}^{(1)} + \chi_{MS}$, obtained by (5) from experimental XANES, permits one to also extract the $\chi_{SS}^{(1)}$ term. The extraction was performed by applying the BFT procedure to $|F(R)|$ of the $\chi_{SS}^{(1)} + \chi_{MS}$ within the first shell R range. In figure 6 the extracted $\chi_{SS}^{(1)}(\varepsilon)$ terms for berlinite (CN $=$ 4) and pyrophyllite (CN $=$ 6) are compared with the theoretical terms, calculated using the diffraction data for the corresponding first shell distances and CN.

5. Determination of interatomic distances and CN

In figure 6(a) the function $\chi_{SS}^{(1)}(\varepsilon)$, extracted from the experimental Al K-XANES in berlinite, is compared with the corresponding theoretical function, calculated as a sum of two terms: $\chi_{SS}^{(1,1)} + \chi_{S}^{(1,)}$, according to the split of the oxygen tetrahedron in berlinite into two subshells with radii $R_{1,j}$ and CN $N_{1,j}$ (j is the number of the subshell): first subshells, ($R_{1,1} = 1.732$ Å with $N_{1,1} = 2$ atoms, and second subshell, $R_{1,2} = 1.745$ Å with $N_{1,2} = 2$ atoms [23]. The same comparison for a pyrophyllite structure, presented in figure 6(b), is carried out with the theoretical function $\chi_{SS}^{(1)}(\varepsilon)$ calculated as a sum of three terms: $\chi_{SS}^{(1,1)} + \chi_{SS}^{(1,)} + \chi_{SS}^{(1,3)}$, according to the split of the oxygen octahedron into three subshells: $R_{1,1} = 1.888$ Å with $N_{1,1} = 2$ atoms, $R_{1,2} = 1.921$ Å with $N_{1,2} = 2$ atoms and $R_{1,1} = 1.926$ Å with $N_{1,1} = 2$ atoms [24].

Table 1. Structure parameters for the first oxygen shell in berlinite and pyrophyllite, obtained from diffraction data and by the proposed method, applied to Al K-XANES.

	Berlinite (CN = 4)		Pyrophyllite (CN = 6)	
	Diffraction [23]	Al K-XANES	Diffraction [24]	Al K-XANES
$R_{1,1}$ (Å)	1.732	1.740	1.888	1.841
$N_{1,1}$	2	4	2	2
$R_{1,2}$ (Å)	1.745		1.921	1.972
$N_{1,2}$	2		2	4
$R_{1,3}$ (Å)			1.926	
$N_{1,3}$			2	

The function $\chi_{SS}^{(1)}(\varepsilon)$, extracted from the experimental XANES, can now be used to determine the values of $R_{1,j}$ and $N_{1,j}$ through the fitting procedure with variable parameters $R_{1,j}$ and $N_{1,j}$. The other parameters usually varied are E_0, Γ and the DW parameter $2\sigma^2$. Within the method of HF MT-potential generation [15], the parameter E_0 is not needed and the photoelectron energies or wave numbers are initiated from the constant interstitial potential E_{MT}. The parameter Γ for extrinsic losses is also not used, since these losses were considered more appropriate for XANES description, exponential form $\exp(-R/\lambda(\varepsilon))$, and as was mentioned in section 2, the $\lambda(\varepsilon)$ was chosen according to [5] via direct XANES calculations. The DW parameter is known to be strongly correlated with CN when the fitting of EXAFS is performed. At the same time, according to the approximation discussed in section 2, the experimental Al K-XANES spectra of berlinite and pyrophyllite were described in [5] within the short range of small XANES energies, under the DW parameter $2\sigma^2 = 0$, and therefore the fitting was performed using the same fixed value. However, the effect of thermal atomic motion on XANES, which rapidly increases with increasing energy, as well as the correlation problem between $2\sigma^2$ and CN within the fitting procedure, are under consideration.

To illustrate the possibilities and the accuracy of the fitting procedure within the short k range considered, it was applied to the theoretical function $\chi_{SS}^{(1,1)}$ of berlinite. The values obtained of $R_{1,1} = 1.732$ Å and $N_{1,1} = 2$ appeared to be the same as their diffraction values, used for the $\chi_{SS}^{(1,1)}$ calculation. The fitting was performed with the central Al-phase shift and the phase shifts and scattering amplitudes on the nearest O-atoms, calculated using the HF MT-potential model for the compounds studied [5].

The results of the fitting, applied to $\chi_{SS}^{(1)}$ functions, extracted from the experimental Al K-XANES of berlinite and pyrophyllite, are presented in table 1. The photoelectron phase shifts and scattering amplitudes on the O-atoms were taken to be the same for all the subshells within each fitting model, which represents the split of the first oxygen shell in the compounds studied.

As can be seen in table 1, the small split value ($\sim$0.01 Å) between the first and the second subshells in berlinite, as well as between the second and the third subshells in the pyrophyllite structures, cannot be distinguished by the fitting code used. For berlinite, this code gives the average value for $R_{1,1}$ and $R_{1,2}$ distances together with the total $N = N_{1,1} + N_{1,2} = 4$ and for pyrophyllite, the second and the third subshells are identified as one subshell at 1.972 Å with the correct total number of atoms = 4. At the same time, a larger split value ($\sim$0.03 Å) between the first and the second subshells in pyrophyllite is reproduced. It must be emphasized that the values obtained for $R_{1,j}$ and $N_{1,j}$, presented in the table, are stable under the variations of their initial or starting values, used for the fitting procedure. For example, the pyrophyllite structure parameters presented in the table can be obtained starting from two different data

sets: (a) $R_{1,1} = 1.7$ Å, $N_{1,1} = 3$, $R_{1,2} = 2.1$ Å, $N_{1,2} = 2$ and (b) $R_{1,1} = 1.7$ Å, $N_{1,1} = 2$, $R_{1,2} = 2.1$ Å, $N_{1,2} = 3$. At the same time, the parameters for the berlinite structure can be obtained starting from both $R_1 = 1.4$ Å, $N_1 = 2$ or $R_1 = 2.1$ Å, $N_1 = 6$ atoms.

6. Summary and conclusions

The results obtained can be summarized in the form of the method for quantitative determination of interatomic distances and CN from experimental K-XANES in crystalline minerals with a distorted local environment of light metallic atoms, based on the following points:

(a) In Al- and Mg-containing minerals, the contribution into the K-XANES spectrum from the photoelectron single-scattering processes on the second and more distant shells (LRO term, $\chi_{SS}^{LRO}\lambda(\varepsilon)$) can be theoretically reproduced with discrepancies of ∼0.3–0.4 Å in the values of the shell radii, using the unambiguous diffraction data on cell unit parameters and the type of point symmetry.

(b) Subtracting the theoretically restored term χ_{SS}^{LRO} from the experimental absorption cross-section $\sigma^{exper}(\varepsilon)$, according to equation (5), one can extract the sum of the first shell term $\chi_{SS}^{(1)}$ and the MS term χ_{MS}, i.e., the function $\chi_{SS}^{(1)}(\varepsilon) + \chi_{MS}(\varepsilon)$.

(c) The Fourier transformation of $\chi_{SS}^{(1)}(\varepsilon) + \chi_{MS}(\varepsilon)$ and the application in series of the BFT procedure with window function to the $|F(R)|$ obtained, permits one to extract the term $\chi_{MS}(\varepsilon)$ and the first shell term $\chi_{SS}^{(1)}(\varepsilon)$ from experimental XANES.

(d) Fitting of the extracted term $\chi_{SS}^{(1)}(\varepsilon)$ by the theoretical terms, simulated within alternative models of the first oxygen shell split under the structure distortions in the environment of the absorbing atom, permits one to obtain the interatomic distances and CN in reasonable quantitative agreement with the diffraction data for the reference compounds.

Further development of the proposed method would be its application to determine the interatomic distances and CN for the light metallic atom environment in gels, glasses and amorphous minerals, when the local structure of this environment is difficult to assess by conventional diffraction methods. In these compounds, the second and more distant shells especially are poorly formed due to the structure disorder. So the main problem under consideration is the theoretical recovery of the χ_{SS}^{LRO} term in equation (5) for these compounds, which is necessary to extract the function $\chi_{SS}^{(1)}(\varepsilon) + \chi_{MS}$ from the experimental XANES.

References

[1] Sircon N, Ravel B, Yacoby Y, Stern E A, Dogan E and Rehr J J 1994 *Phys. Rev.* B **50** 13 168–80
[2] Bugaev L A, Shuvaeva V A, Alekseenko I B, Zhuchkov K N and Husson E 1997 *J. Physique* IV **7** 179–81
[3] Knapp G S, Veal B W, Pan H K and Klippert T 1982 *Solid State Commun.* **44** 1343–5
[4] Ildefonse Ph, Cabaret D, Sainctavit Ph, Calas G, Flank A-M and Lagarde P 1998 *Phys. Chem. Min.* **25** 112–21
[5] Bugaev L A, Ildefonse Ph, Flank A-M, Sokolenko A P and Dmitrienko H V 1998 *J. Phys.: Condens. Matter* **10** 5463–73
[6] Natoli C R, Misemer D K, Doniach S and Kutzler F W 1980 *Phys. Rev.* A **22** 1104–6
[7] Vedrinskii R V, Bugaev L A, Gegusin I I, Kraizman V L, Novakovich A A, Ruus R, Maiste A and Elango M A 1982 *Solid State Commun.* **44** 1401–7
[8] Durham F J, Pendry J B and Hodges C H 1982 *Comp. Phys. Commun.* **25** 193–205
[9] Gurman S J, Binstead N and Ross I 1984 *J. Phys.: Condens. Matter* **17** 143–51
[10] Bugaev L A, Shuvaeva V A, Rusakova E B and Alekseenko I B 1999 *J. Synchrotron. Rad.* **6** 299–301
[11] Ildefonse Ph, Calas G, Flank A-M and Lagarde P 1995 *Nuclear Instruments and Methods in Physics Research* B **95** 172–5
[12] Gibbs N 1971 *Am. Mineral.* **56** 791–825
[13] Fisher P 1967 *Z. Kristallogr.* **124** 275–302

[14] Vedrinskii R V, Bugaev L A and Levin I G 1988 *Phys. Status Solidi* b **150** 307–14
[15] Bugaev L A, Vedrinskii R V, Levin I G and Airapetian V M 1991 *J. Phys.: Condens. Matter* **3** 8967–79
[16] Vedrinskii R V, Bugaev L A and Airapetian V M 1991 *J. Phys. B: At. Mol. Phys.* **24** 1967–75
[17] Vedrinskii R V, Bugaev L A and Levin I G 1989 *Physica* B **158** 421–4
[18] Bugaev L A and Vedrinskii R V 1985 *Phys. Status Solidi* **132** 459–64
[19] Rehr J J, Bardyszewski W and Hedin L *J. Physique* IV **7** 97–8
[20] Bugaev L A, Ildefonse Ph, Flank A-M and Sokolenko A P to be published
[21] Feldman L C and Mayer J W 1986 *Fundamentals of Surface and Thin Films Analysis* (Amsterdam: North-Holland) p 342
[22] Rupp B, Smith B and Wong J 1992 *Comp. Phys. Commun.* **67** 543–9
[23] Schwarzenbach von D 1966 *Z. Kristallogr.* **123** 161–85
[24] Lee J H and Gugggenheim S 1981 *Am. Mineral.* **66** 350–7
[25] Cabaret D, Ildefonse Ph, Sainctavit Ph and Flank A M 1998 *Am. Mineral.* **85** 300–4